Sun Sensor Model

Nikolas Trawny and Stergios Roumeliotis
Department of Computer Science & Engineering
University of Minnesota

Center for
Distributed Robotics

Technical Report
Number -2005-001
January 2005

Dept. of Computer Science & Engineering
University of Minnesota
4-192 EE/CS Building
200 Union St. S.E.
Minneapolis, MN 55455
Tel: (612) 625-2217
Fax: (612) 625-0572
URL: http://www.cs.umn.edu/~trawny

Sun Sensor Model

Nikolas Trawny and Stergios Roumeliotis
Department of Computer Science & Engineering
University of Minnesota

Robotics & Autonomous Systems Laboratory, TR-2005-001
January 2005

1 Pin-hole Camera Model

The Sun Sensor is represented mathematically by the simple pin-hole camera model, depicted in figure 1. We attach the sensor coordinate frame S to the aperture, with the z-axis pointing outward along the boresight. The focal length f describes the distance between its origin and the image plane.

In this model, the vector $\mathbf{r}_\odot$, pointing from the pin-hole to the sun, and $\mathbf{a}$, pointing from the pin-hole to the image of the sun on the image plane, are obviously collinear.

After normalizing, we can establish the following equality

$$\mathbf{r_0} = \frac{\mathbf{r}_\odot}{|\mathbf{r}_\odot|} = -\frac{\mathbf{a}}{|\mathbf{a}|} \tag{1}$$

The attitude information of the Sun Sensor measurement lies in the fact that we know the position of the sun in a global coordinate frame $\{G\}$, whereas we can measure a projection of the unit vector pointing towards the sun in the Sun Sensor's coordinate frame $\{S\}$.

$$^G\mathbf{P}_\odot = {}^G\mathbf{P}_{S_{Org}} + {}^G_S\mathbf{C}\,{}^S\mathbf{r}_\odot \tag{2}$$

$$^S\mathbf{r}_\odot = {}^S_G\mathbf{C}\left({}^G\mathbf{P}_\odot - {}^G\mathbf{P}_{S_{Org}}\right) = {}^S_G\mathbf{C}\,{}^G\mathbf{r}_\odot \tag{3}$$

For now, the position of the spacecraft (and thus the position of the Sun Sensor ${}^G\mathbf{P}_{S_{Org}}$) is assumed to be known, which in turn implies knowledge of ${}^G\mathbf{r}_\odot$.

The rotation between the global and the sensor frame can be decomposed into two rotational matrices

$${}^S_G\mathbf{C} = {}^S_R\mathbf{C}\,{}^R_G\mathbf{C} \tag{4}$$

where the transformation ${}^S_R\mathbf{C}$ between sensor frame $\{S\}$ and spacecraft frame $\{R\}$ is known and fixed, and the transformation ${}^R_G\mathbf{C}$ is a function of the attitude quaternion.

The actual measurement $\mathbf{z}$ will be a projection of the normalized vector $\mathbf{r_0}$, corrupted by zero-mean, white, Gaussian noise η

$$\mathbf{z} = \mathbf{\Pi}\,{}^S_R\mathbf{C}\,{}^R_G\mathbf{C}\,{}^G\mathbf{r_0} + \eta \tag{5}$$

where $\mathbf{\Pi}$ is the projection matrix.

For the update phase of the Kalman filter, we need to relate the measurement error $\tilde{\mathbf{z}}$ to the state vector.

$$\tilde{\mathbf{z}} = \mathbf{z} - \tilde{\mathbf{z}} = \mathbf{\Pi}\,{}^S_R\mathbf{C}\left({}^R_G\mathbf{C}(q) - {}^R_G\mathbf{C}(\hat{q})\right)\cdot {}^G\mathbf{r_0} + \eta \tag{6}$$

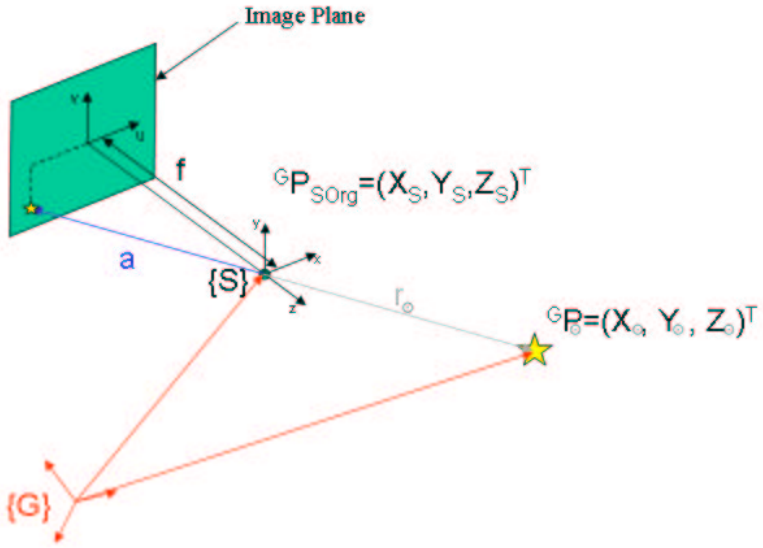

Figure 1: The sun sensor, modelled as a pin-hole camera

Using

$$q = \delta q \otimes \hat{q} \tag{7}$$

$$\begin{aligned} {}^R_G\mathbf{C}(q) &= {}^R_G\mathbf{C}(\delta q \otimes \hat{q}) \\ &= {}^R_G\mathbf{C}(\delta q) \cdot {}^R_G\mathbf{C}(\hat{q}) \end{aligned} \tag{8}$$

$$\begin{aligned} {}^R_G\mathbf{C}(\delta q) &= (2\delta q_4^2 - 1)\mathbf{I}_{3\times 3} - 2\delta q_4 \cdot \lfloor \delta\mathbf{q} \times \rfloor + 2\delta\mathbf{q}\delta\mathbf{q}^{\mathrm{T}} \\ &\quad \text{with } \delta q_4 \approx 1, \quad \delta\mathbf{q} \text{ small} \\ {}^R_G\mathbf{C}(\delta q) &\approx \mathbf{I}_{3\times 3} - 2\lfloor \delta\mathbf{q} \times \rfloor, \quad \text{but } \delta\mathbf{q} = \frac{1}{2}\delta\theta \\ {}^R_G\mathbf{C}(\delta q) &\approx \mathbf{I} - \lfloor \delta\theta \times \rfloor \end{aligned} \tag{9}$$

we can write

$$\tilde{\mathbf{z}} = \mathbf{\Pi}^S_R\mathbf{C} \left({}^R_G\mathbf{C}(\delta q) - \mathbf{I}\right) {}^R_G\mathbf{C}(\hat{q}) \cdot {}^G\mathbf{r_0} + \eta \tag{10}$$

$$\approx \mathbf{\Pi}^S_R\mathbf{C} \left(-\lfloor \delta\theta \times \rfloor\right) {}^R_G\mathbf{C}(\hat{q}) \cdot {}^G\mathbf{r_0} + \eta \tag{11}$$

$$= \mathbf{\Pi}^S_R\mathbf{C} \lfloor {}^R_G\mathbf{C}(\hat{q}) {}^G\mathbf{r_0} \times \rfloor \cdot \delta\theta + \eta \tag{12}$$

$$= \begin{bmatrix} \mathbf{\Pi}^S_R\mathbf{C} \lfloor {}^R_G\mathbf{C}(\hat{q}) {}^G\mathbf{r_0} \times \rfloor & \mathbf{0} \end{bmatrix} \cdot \begin{bmatrix} \delta\theta \\ \tilde{\mathbf{b}} \end{bmatrix} + \eta \tag{13}$$

We will now look at the geometric interpretation of the measurement vector $\mathbf{z}$ and the unit vector ${}^S\mathbf{r_0}$, expressed in the Sun Sensor frame $\{S\}$. Henceforth, we will only consider vectors expressed in the sensor frame and omit the leading superscript ^{S} for notational clarity. The vector $\mathbf{r_0}$ can be parameterized by the image coordinates u,v and f or the angles α_x and α_y.

If we write the components of $\mathbf{r_0}$ and $\mathbf{a}$ as

$$\mathbf{r}_\odot = \begin{bmatrix} r_x \\ r_y \\ r_z \end{bmatrix} \quad \mathbf{a} = \begin{bmatrix} u \\ v \\ -f \end{bmatrix} \tag{14}$$

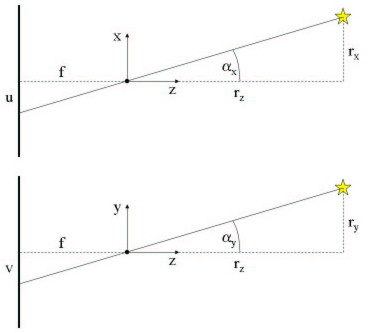

Figure 2: Projection of $\mathbf{r}$ and $\mathbf{a}$

we can, using the collinearity of $\mathbf{r_0}$ and $\mathbf{a}$ and the properties of the projected similar triangles (cf. Fig. 2), establish the relationship

$$\frac{r_x}{r_z} = \frac{u}{-f} \Leftrightarrow u = -f\frac{r_x}{r_z} \tag{15}$$

$$\frac{r_y}{r_z} = \frac{v}{-f} \Leftrightarrow v = -f\frac{r_y}{r_z} \tag{16}$$

We can define the angles α_x and α_y as shown in figure 2 by

$$\tan\alpha_x = \frac{r_x}{r_z} = -\frac{u}{f}, \quad \tan\alpha_y = \frac{r_y}{r_z} = -\frac{v}{f} \tag{17}$$

yielding

$$u = -f\tan\alpha_x, \quad v = -f\tan\alpha_y \tag{18}$$

$$\alpha_x = \arctan(-\frac{u}{f}), \quad \alpha_y = \arctan(-\frac{v}{f}) \tag{19}$$

From equation (1) we can now write the unit vector from the sensor towards the sun as

$$\mathbf{r_0} = \frac{1}{\sqrt{u^2+v^2+f^2}}\begin{bmatrix}-u\\-v\\f\end{bmatrix} = \frac{1}{\sqrt{\tan^2\alpha_x+\tan^2\alpha_y+1}}\begin{bmatrix}\tan\alpha_x\\\tan\alpha_y\\1\end{bmatrix} \tag{20}$$

Note that while α_x could be interpreted as the azimuth, α_y does not exactly correspond to the elevation ϕ (cf. Fig. 3). However, they are closely related and we can write

$$\mathbf{r}_\odot = |\mathbf{r}_\odot|\begin{bmatrix}\cos\phi\sin\alpha_x\\\sin\phi\\\cos\phi\cos\alpha_x\end{bmatrix} \tag{21}$$

Obviously, $\frac{r_x}{r_z} = \tan\alpha_x$ but $\frac{r_y}{r_z} = \tan\alpha_y = \tan\phi/\cos\alpha_x$.

In accordance with the measurement model (eq. (5)), the actual measurement $\mathbf{z}$ will be a projection of $\mathbf{r_0}$ on the $2D$-plane, for example according to

$$\mathbf{z} = \mathbf{\Pi}\cdot\mathbf{r_0}+\eta, \qquad \mathbf{\Pi} = \begin{bmatrix}1&0&0\\0&1&0\end{bmatrix} \tag{22}$$

$$= \frac{1}{\sqrt{(\tan\alpha_x)^2+(\tan\alpha_y)^2+1}}\begin{bmatrix}\tan\alpha_x\\\tan\alpha_y\end{bmatrix}+\eta \tag{23}$$

$$= \frac{1}{\sqrt{u^2+v^2+f^2}}\begin{bmatrix}-u\\-v\end{bmatrix}+\eta \tag{24}$$

In a next step, we will have to determine the covariance of the measurement noise η.

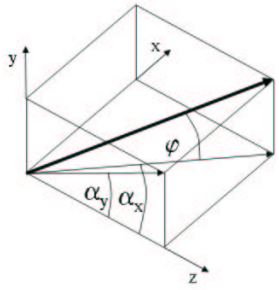

Figure 3: Relationship of α_x, α_y and elevation ϕ

2 Errormodel

For a real measurement, we will have to replace the values of u and v or of α_x and α_y by their respective measured values u_m, v_m or α_{xm}, α_{ym}. We can assume that they correspond to the real values, corrupted by zero-mean, white, Gaussian noise. We can furthermore assume, that u_m and v_m are functions of some internal camera parameters $\mathbf{\Theta}$ which are also error-corrupted.

$$u_m(\mathbf{\Theta}) = u + n_u, \quad v_m(\mathbf{\Theta}) = v + n_v \tag{25}$$

$$\alpha_{xm} = \alpha_x + n_{\alpha_x}, \quad \alpha_{ym} = \alpha_y + n_{\alpha_y} \tag{26}$$

$$\mathbf{n_{u,v}} = \begin{bmatrix} n_u \\ n_v \end{bmatrix}, \quad \mathbf{n}_\alpha = \begin{bmatrix} n_{\alpha_x} \\ n_{\alpha_y} \end{bmatrix} \tag{27}$$

We now have $\mathbf{z}$ as non-linear functions of the true vector $\mathbf{r_0}$ and the noise $\mathbf{n_{u,v}}$ or $\mathbf{n}_\alpha$. By linearizing around the true vector $\mathbf{r_0}$, we can obtain a relationship of the form in eq. (5). We will first show this for noise in α_x and α_y.

In the following two sections, we tacitly assume that the linearizations are evaluated at $\mathbf{n_{u,v}} = \mathbf{n}_\alpha = 0$. In reality, this will be unrealizable, and the true values for u, v or α_x, α_y will have to be replaced by their measured counterparts u_m, v_m or α_{xm} and α_{ym}, respectively.

2.1 Measurement Noise in terms of Noise in α_x and α_y

Here, we linearize $\mathbf{z}$ around the true α_x and α_y:

$$\mathbf{z} = \mathbf{h}(\alpha_x, \alpha_y, \mathbf{n}_\alpha) = \frac{1}{\sqrt{(\tan\alpha_{xm})^2 + (\tan\alpha_{ym})^2 + 1}} \begin{bmatrix} \tan\alpha_{xm} \\ \tan\alpha_{ym} \end{bmatrix} \tag{28}$$

$$\approx \frac{1}{\sqrt{(\tan\alpha_x)^2 + (\tan\alpha_y)^2 + 1}} \begin{bmatrix} \tan\alpha_x \\ \tan\alpha_y \end{bmatrix} + \mathbf{\Gamma}_\alpha \cdot \mathbf{n}_\alpha \tag{29}$$

where

$$\mathbf{\Gamma}_\alpha = \frac{\partial \mathbf{h}}{\partial \mathbf{n}_\alpha} \tag{30}$$

Comparison to eq. (23) shows

$$\eta \approx \mathbf{\Gamma}_\alpha \cdot \mathbf{n}_\alpha \tag{31}$$

The jacobian $\mathbf{\Gamma}_\alpha$ is computed in terms of α_x and α_y as

$$\begin{aligned}\mathbf{\Gamma}_\alpha(\alpha_x,\alpha_y) &= \frac{1}{((\tan\alpha_x)^2+(\tan\alpha_y)^2+1)^{\frac{3}{2}}}\cdot \\ &\cdot\begin{bmatrix}(\tan^2\alpha_y+1)(\tan^2\alpha_x+1) & -(\tan\alpha_x\tan\alpha_y)(\tan^2\alpha_y+1)\\ -(\tan\alpha_x\tan\alpha_y)(\tan^2\alpha_x+1) & (\tan^2\alpha_x+1)(\tan^2\alpha_y+1)\end{bmatrix} \qquad (32)\\ &= \frac{1}{(lm-n^2)^{\frac{3}{2}}}\begin{bmatrix}lm & -nm\\ -nl & lm\end{bmatrix} \qquad (33)\end{aligned}$$

where we introduced the following abbreviations

$$l=(\tan^2\alpha_x+1),\quad m=(\tan^2\alpha_y+1),\quad n=(\tan\alpha_x\tan\alpha_y) \qquad (34)$$

Using the definitions of α_x and α_y (cf. eq. (17)), we can also express $\mathbf{\Gamma}_\alpha$ in terms of image coordinates u and v:

$$\mathbf{\Gamma}_\alpha(u,v)=\frac{1}{f\,(u^2+v^2+f^2)^{\frac{3}{2}}}\begin{bmatrix}(v^2+f^2)(u^2+f^2) & -(uv)(v^2+f^2)\\ -(uv)(u^2+f^2) & (v^2+f^2)(u^2+f^2)\end{bmatrix} \qquad (35)$$

Since $\mathbf{n}_\alpha$ is assumed to be zero-mean, η is also zero-mean, and we can now compute its covariance as

$$\begin{aligned}\mathrm{cov}(\eta) &= \mathrm{E}\left(\eta\,\eta^{\mathrm{T}}\right) &(36)\\ &= \mathrm{E}\left(\mathbf{\Gamma}_\alpha\mathbf{n}_\alpha\,{\mathbf{n}_\alpha}^{\mathrm{T}}\mathbf{\Gamma}_\alpha^{\mathrm{T}}\right) &(37)\\ &= \mathbf{\Gamma}_\alpha\,\mathrm{cov}(\mathbf{n}_\alpha)\mathbf{\Gamma}_\alpha^{\mathrm{T}} &(38)\end{aligned}$$

In order to determine $\mathrm{cov}(\mathbf{n}_\alpha)$ from an experiment, we measure $\mathrm{cov}(\eta)$ for a test point with $\alpha_x=\alpha_y=0$ that should project to the center of the image plane. In reality, due to intrinsic camera errors, the point will project around the center of the image plane, and we can measure the error and determine its covariance $\mathrm{cov}(\eta)$. In this case,

$$\mathbf{\Gamma}_\alpha(\alpha_x=\alpha_y=0)=\mathbf{I} \qquad (39)$$

and we can conclude that

$$\mathrm{cov}(\mathbf{n}_\alpha)=\mathrm{cov}(\eta)|_{\alpha_x=\alpha_y=0} \qquad (40)$$

Having thus found $\mathrm{cov}(\mathbf{n}_\alpha)$, we can compute the covariance of η at any other point by applying eq. (38).

If we assume uncorrelated errors with equal variance for α_x and α_y then

$$\mathrm{cov}(\mathbf{n}_\alpha)=\sigma^2\mathbf{I} \qquad (41)$$

and

$$\begin{aligned}\mathrm{cov}(\eta) &= \sigma^2\mathbf{\Gamma}_\alpha\mathbf{\Gamma}_\alpha^{\mathrm{T}} &(42)\\ &= \sigma^2\frac{1}{(lm-n^2)^3}\begin{bmatrix}m^2(l^2+n^2) & -lmn(l+m)\\ -lmn(l+m) & l^2(m^2+n^2)\end{bmatrix} &(43)\end{aligned}$$

where we have again made use of the abbreviations (34).

Due to the linearization in eq. (29), this is an approximation for the actual covariance of the noise. However, a Monte Carlo simulation, in which we have computed the sample covariance of the true η as determined by the difference between eq. (23) and eq. (28) (cf. Fig. 4), shows good correspondence.

In a next step, we will show that $\mathrm{cov}(\eta)$ is positive definite. Its determinant is computed as

$$\begin{aligned}\det\left(\mathrm{cov}(\eta)\right) &= \det\left(\sigma^2\mathbf{\Gamma}_\alpha\mathbf{\Gamma}_\alpha^{\mathrm{T}}\right) &(44)\\ &= \frac{\sigma^4}{(lm-n^2)^6}\left(m^2(l^2+n^2)l^2(m^2+n^2)-(lmn(l+m))^2\right) &(45)\\ &= \frac{\sigma^4}{(lm-n^2)^4}\left(l^2m^2\right) &(46)\end{aligned}$$

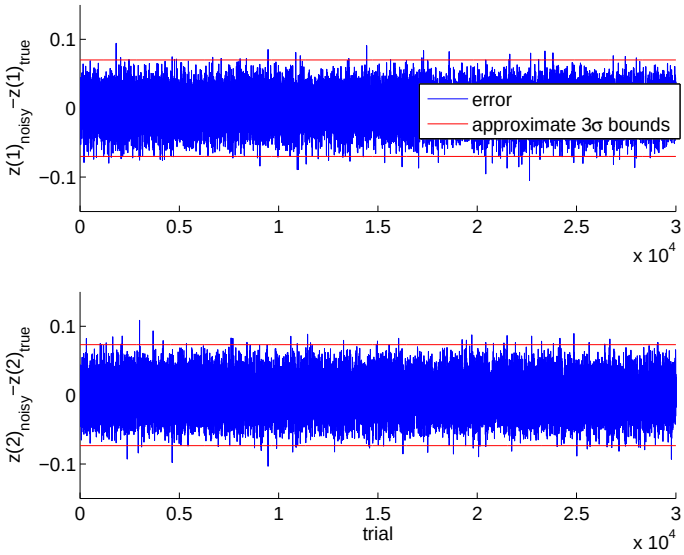

Figure 4: True η for $\alpha_x = \pi/4$, $\alpha_y = pi/6$ and $\sigma = 0.03$, with approximate 3σ-bounds computed from eq. (43)

Now, since

$$\tan^2 \alpha_x \geqslant 0, \quad \tan^2 \alpha_y \geqslant 0 \tag{47}$$

$$\Rightarrow \quad l > 0, \quad m > 0, \quad lm - n^2 = \tan^2 \alpha_x + \tan^2 \alpha_y + 1 > 0 \tag{48}$$

we conclude that

$$\text{trace}(\text{cov}(\eta)) \geqslant 0, \quad \det(\text{cov}(\eta)) > 0 \tag{49}$$

and therefore $\text{cov}(\eta)$ is positive definite

$$\text{cov}(\eta) \succ 0 \tag{50}$$

The eigenvalues of $\text{cov}(\eta)$ are computed as

$$\det(\lambda \mathbf{I} - \sigma^2 \mathbf{\Gamma}_\alpha \mathbf{\Gamma}_\alpha^{\mathrm{T}}) = 0 \tag{51}$$

$$\Leftrightarrow \quad \lambda_{1/2} = \frac{\sigma^2}{(lm - n^2)^3} \left(\frac{l^2n^2 + 2l^2m^2 + m^2n^2}{2} \pm \sqrt{\frac{(l^2n^2 + 2l^2m^2 + m^2n^2)^2 - (2l^2m^2 - 2lmn^2)^2}{4}} \right) \tag{52}$$

From eq. (48) and by inspection, the discriminant is not only ensured to be positive, but also the eigenvalues can be seen to be both positive, thus confirming positive definiteness.

2.2 Measurement Noise in terms of Noise in u and v

Completely analogous to the above procedure, we can also express $\mathbf{z}$ as a non-linear function of the image coordinates u, v and the internal camera parameters $\mathbf{\Theta}$. Similar to eq. (29), we can then linearize around the true image coordinates and write

$$\mathbf{z} \quad = \quad \mathbf{h}\left(u, v, \mathbf{\Theta}, \mathbf{n}_{\mathbf{u},\mathbf{v}}\right) = \frac{1}{\sqrt{u_m^2 + v_m^2 + f^2}} \begin{bmatrix} -u_m \\ -v_m \end{bmatrix} \tag{53}$$

$$\approx \quad \frac{1}{\sqrt{u^2 + v^2 + f^2}} \begin{bmatrix} -u \\ -v \end{bmatrix} + \mathbf{\Gamma}_{u,v} \left(\mathbf{D} \cdot \tilde{\mathbf{\Theta}} + \mathbf{n}_{\mathbf{u},\mathbf{v}} \right) \tag{54}$$

where

$$\mathbf{\Gamma}_{u,v} = \frac{\partial \mathbf{h}}{\partial \begin{bmatrix} u_m, & v_m \end{bmatrix}^{\mathrm{T}}} \tag{55}$$

and

$$\mathbf{D} = \frac{\partial \begin{bmatrix} u_m, & v_m \end{bmatrix}^{\mathrm{T}}}{\partial \mathbf{\Theta}} \tag{56}$$

Now,

$$\eta \approx \mathbf{\Gamma}_{u,v} \left(\mathbf{D} \cdot \tilde{\mathbf{\Theta}} + \mathbf{n}_{\mathbf{u},\mathbf{v}} \right) \tag{57}$$

and

$$\mathbf{\Gamma}_{u,v} = \frac{1}{(u^2+v^2+f^2)^{\frac{3}{2}}} \begin{bmatrix} -(v^2+f^2) & uv \\ uv & -(u^2+f^2) \end{bmatrix} \tag{58}$$

which is not the same as eq. (35) but related to it. Using the definition of $\mathbf{n}_\alpha$ in eq. (27) and (26), and using the definition of α_x and α_y in eq. (19), we can write

$$\begin{aligned} \mathbf{\Gamma}_{u,v} &= \frac{\partial \mathbf{h}}{\partial \mathbf{n}_{\mathbf{u},\mathbf{v}}} && (59) \\ &= \frac{\partial \mathbf{h}}{\partial \mathbf{n}_\alpha} \cdot \frac{\partial \mathbf{n}_\alpha}{\partial \mathbf{n}_{\mathbf{u},\mathbf{v}}} && (60) \\ &= \mathbf{\Gamma}_\alpha(u,v) \cdot \begin{bmatrix} -\frac{f}{f^2+u^2} & 0 \\ 0 & -\frac{f}{f^2+v^2} \end{bmatrix} && (61) \end{aligned}$$